

## Theory of collisional transfer between orientation and alignment of atoms excited by a single-mode laser

T. Manabe, T. Yabuzaki, and T. Ogawa

*Ionosphere Research Laboratory, Kyoto University, Uji, Kyoto, Japan*

(Received 20 March 1979)

Theoretical study is made of the transfer between orientation and alignment of excited-state atoms by anisotropic collisions with ground-state atoms. The anisotropy considered is due to the anisotropic velocity distribution of atoms excited by a single-mode laser beam. The transfer rate and relaxation rates for each multipole moment are calculated for the excited state with  $J = 1$  as a function of detuning of the laser frequency from the center of an absorption line and mass of perturbing ground-state atoms. Experiments to observe the transfer from alignment to orientation and from orientation to alignment in a weak magnetic field are considered, and corresponding signals are analyzed in terms of the transfer and relaxation rates.

### I. INTRODUCTION

Collisional relaxation among Zeeman substates of the excited states of atoms has been extensively studied theoretically and experimentally in past two decades.<sup>1</sup> In most of these experiments, the atoms are excited by the light from a spectral lamp or by collisions with electrons, so that the velocity distribution of excited atoms is generally given by the Maxwellian function, when self-absorption can be neglected. As a result, the collisions of the excited (emitter) atoms with the ground-state (perturber) atoms are isotropic, i.e., all collision directions are equally probable. It is obvious from the argument of symmetry that isotropic collisions cause the independent relaxation of each multipole moment such that

$$\frac{d\rho_q^k}{dt} = -\Gamma^k \rho_q^k, \quad (1)$$

where  $\rho_q^k$  is the density-matrix element corresponding to the  $q$  component ( $q = -k, -k+1, \dots, +k$ ) of the  $2^k$ -pole moment of the excited state, i.e.,  $\rho_0^0$  is the population,  $\rho_q^1$  is the magnetic dipole moment or "orientation,"  $\rho_q^2$  is the electric quadrupole moment or "alignment," and so on. Equation (1) also shows that the relaxation rate is independent of the value of  $q$ . In recent years, gas lasers have been used to study the relaxation of orientation and alignment of laser levels,<sup>2</sup> and now tunable lasers such as dye lasers are considered to be powerful light sources because they remove the limitation on the levels to be studied. When atoms are excited by laser light, the velocity distribution of excited atoms along the light axis is generally different from the Maxwellian function, whose width is given by the gas temperature.

In the present paper, we would like to give the theory of relaxation of atoms excited by a single-mode laser light. By such excitation the velocity

distribution of excited emitters along the light axis generally becomes narrower than the distributions perpendicular to the light axis, which are given by a Maxwellian function. Consequently the collisions with perturber atoms become anisotropic, and the anisotropy can be changed by the detuning of the laser frequency from the absorption line center. In case of anisotropic collisions, the change in  $\rho_q^k$  is no longer given by Eq. (1) and can generally be expressed as

$$\frac{d\rho_q^k}{dt} = -\sum_{k'q'} \Gamma_{qq'}^{kk'} \rho_q^{k'}, \quad (2)$$

which shows that the transfer among multipole moments becomes possible. We have calculated  $\Gamma_{qq'}^{kk'}$  by changing the laser tuning relative to the line center for various masses of perturber atoms, assuming that the interaction between colliding atoms is electric dipole-dipole in the same manner as the isotropic-collision theories of Omont,<sup>3</sup> and Berman and Lamb.<sup>4</sup> Although we have analyzed for the single-mode excitation, the results obtained are easily applicable to excitation by light with an arbitrary spectrum. We discuss also the relations of  $\Gamma_{qq'}^{kk'}$  with observable quantities in the Hanle experiment using linearly polarized or circularly polarized laser light. Such experiments are now under way in our laboratory using neon atoms in the  $2p_4$  state excited by a single-mode dye laser. We have obtained preliminary results for the signal of orientation transferred from alignment by collisions with ground-state neon atoms. The precise experimental results may be reported elsewhere.

### II. ASSUMPTIONS AND APPROXIMATIONS

We consider binary collisions between an excited atom (emitter) to be observed and a perturber atom in its nondegenerate ground state

( $J=0$ ). As in the conventional theory of isotropic collisions,<sup>3,4</sup> several approximations are made: (i) The relative trajectory of a perturber is assumed to be a straight-line path. (ii) The electric dipole-dipole approximation is made for the emitter-perturber interaction, and we shall restrict ourselves to its lowest-order contribution, that is, to the first order for resonant collisions and to the second order for nonresonant collisions. (iii) We assume that the duration of the collisional interaction is much smaller than the time between binary collisions (impact approximation). (iv) External magnetic field is assumed to be weak so that the Larmor precession of the excited state can be neglected during the collisional interaction. (v) Collisions are assumed to be nonadiabatic with respect to Zeeman substates.

We use a reference frame  $\Omega_0$  in which the emitter is fixed at the origin, the perturber moves with relative velocity  $\vec{v}_R$  in the  $z_c$  direction, and the impact parameter  $\vec{b}$  is directed to the  $x_c$  axis as seen in Fig. 1. [This is the same frame as Cooper's ( $x', y', z'$ ) frame.<sup>5</sup> To transfer from Berman's collision frame<sup>4</sup> to ours, a rotation of  $(\pi, \frac{1}{2}\pi, \pi)$  is required.]

We define the time evolution matrix  $M(t)$  of the state vector  $\vec{a}$  in the interaction representation, where the state vector  $\vec{a}$  is the direct product of the excited-state state vector of the emitter and the ground-state state vector of the perturber in the interaction representation as defined in Eq. (53) of Ref. 4. Since we consider only the case where the ground state of the perturber is nondegenerate, the vector  $\vec{a}$  is composed of  $2j+1$  elements  $a_m$  ( $m=j, \dots, -j$ ), where  $j$  is the total angular momentum of the excited state of the emitter and  $m$  is the magnetic quantum number. The time evolution of  $\vec{a}$  is given by

$$\vec{a}(t) = M(t)\vec{a}(-\infty). \quad (3)$$

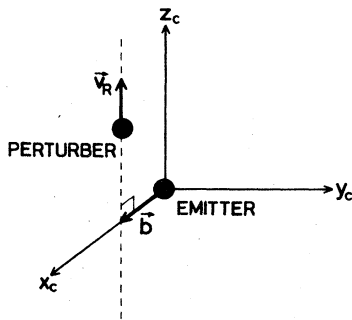


FIG. 1. Reference frame  $\Omega_0$  where the emitter is fixed at the origin and the perturber moves with relative velocity  $\vec{v}_R$  in the  $z_c$  direction. The  $x_c$  axis is chosen in the direction of the impact parameter  $\vec{b}$ .

We define the density matrix of the emitter-perturber system, in which the emitter is in its excited state and the perturber is in its ground state, as  $\rho_{mm'} = a_m a_{m'}^*$ . The change in the density matrix caused by a collision in our reference frame is

$$\delta\rho_{mm'}(b, v_R, \Omega_0, c) = \sum_{nn'} M_{mm'}^{nn'}(b, v_R, \Omega_0) \rho_{nn'}(c), \quad (4)$$

where

$$M_{mm'}^{nn'}(b, v_R, \Omega_0) = M_{mn}(\infty) M_{m'n'}^*(\infty) - \delta_{mn} \delta_{m'n'}, \quad (5)$$

and  $c$  is the past-collision history. Since we use the impact approximation, which implies that each collision is an independent event,  $M_{mm'}^{nn'}(b, v_R, \Omega_0)$  is not affected by past-collision histories. Hence the averaging of Eq. (4) over all possible histories is performed by replacing  $\rho_{nn'}(c)$  with its average over all possible histories, which is denoted by  $\rho_{nn'}$ .

### III. RELAXATION AND TRANSFER RATES OF ALIGNMENT AND ORIENTATION

#### A. Collisions of emitters moving with a definite velocity

Before considering the case in which emitters are excited by a single-mode laser beam, we will consider here particular collisions where emitters have a definite velocity  $\vec{v}_e$  in a particular direction, while perturbers have an isotropic Maxwellian velocity distribution. We consider a new frame ( $X, Y, Z$ ) which moves with the velocity  $\vec{v}_e$  in the  $Z$  direction such that the emitter is fixed at the origin. As shown in Fig. 2, we can transform ( $x_c, y_c, z_c$ ) to ( $X, Y, Z$ ) by a rotation  $\Omega_1 = (\frac{1}{2}\pi - \phi, \theta, -\frac{1}{2}\pi - \psi)$ , where  $\theta$  is the angle between  $\vec{v}_e$  and the relative velocity  $\vec{v}_R$ . Since perturber velocity is given by  $\vec{v}_p = \vec{v}_e + \vec{v}_R$ , the perturber velocity distribution (assumed to be isotropic Maxwellian) is

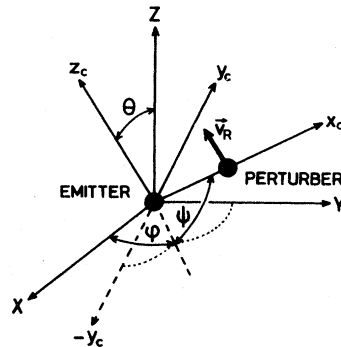


FIG. 2. Relationship between the reference frame ( $x_c, y_c, z_c$ ) and the frame ( $X, Y, Z$ ) where the emitter velocity  $\vec{v}_e$  is fixed in the  $Z$  direction.

given by

$$f_p(\vec{v}_e + \vec{v}_R) = (\alpha_p/\pi)^{3/2} \exp[-\alpha_p(v_e^2 + v_R^2 + 2v_e v_R \cos\theta)], \quad (6)$$

where  $\alpha_p = m_p/2kT$ ,  $m_p$  is the mass of the perturber,  $k$  is the Boltzmann constant, and  $T$  is the absolute gas temperature. For fixed  $\vec{v}_e$ , averaging  $M_{mm'}^{nn'}(b, v_R, \Omega_0)$  over the impact parameter and over the relative velocity, we obtain

$$\begin{aligned} \bar{\Gamma}_{mm'}^{nn'}(v_e) &= n_p \sum_{\substack{\mu \mu' \\ \nu \nu'}} \int_0^\infty db \int d^3v_R b v_R f_p(\vec{v}_e + \vec{v}_R) \mathfrak{D}_{\nu\nu'}^{j*}(\Omega_1) \\ &\quad \times \mathfrak{D}_{m'\mu'}^{j*}(\Omega_1) \mathfrak{D}_{m\mu}^j(\Omega_1) \mathfrak{D}_{m\mu}^j(\Omega_1) \\ &\quad \times M_{\mu\mu'}^{\nu\nu'}(b, v_R, \Omega_0), \end{aligned} \quad (7)$$

where  $n_p$  is the perturber density and  $\mathfrak{D}_{m\mu}^j(\Omega_1)$  is the rotation matrix for the rotation  $\Omega_1$ . Using the relation of the Clebsch-Gordan series<sup>6</sup> and 3-j symbols, we can rewrite Eq. (7) as

$$\begin{aligned} \bar{\Gamma}_{mm'}^{nn'}(v_e) &= \sum (-1)^{n-\nu+m'-\mu'} (2J+1)(2J'+1)(2K+1) \begin{bmatrix} j & j & J \\ n & -n' & M \end{bmatrix} \begin{bmatrix} j & j & J \\ \nu & -\nu' & N \end{bmatrix} \begin{bmatrix} j & j & J' \\ m & -m' & M' \end{bmatrix} \\ &\quad \times \begin{bmatrix} j & j & J' \\ \mu & -\mu' & N' \end{bmatrix} \begin{bmatrix} J & J' & K \\ -M & M' & Q \end{bmatrix} \begin{bmatrix} J & J' & K \\ -N & N' & Q' \end{bmatrix} \int_0^\infty db \int d^3v_R n_p b v_R f_p(\vec{v}_e + \vec{v}_R) \mathfrak{D}_{QQ'}^K(\Omega_1) M_{\mu\mu'}^{\nu\nu'}(b, v_R, \Omega_0), \end{aligned} \quad (8)$$

where the summation is taken over  $\mu, \mu', \nu, \nu', M, M', N, N', J, J', K, Q$ , and  $Q'$ .

Owing to the axial symmetry of our system, it is convenient to represent the density matrix on the basis of normalized irreducible tensors.<sup>7-9</sup> Using this representation, we can write the average

collisional relaxation of the density matrix as

$$\frac{d\rho_q^h}{dt} = - \sum_{h'q'} \bar{\Gamma}_{qq'}^{hh'}(v_e) \rho_{q'}^{h'}, \quad (9)$$

and the coefficient of relaxation as

$$\begin{aligned} \bar{\Gamma}_{qq'}^{hh'}(v_e) &= - \sum (-1)^{h+h'-q+\nu-\mu'} [(2k+1)(2k'+1)]^{1/2} (2K+1) \begin{bmatrix} j & j & k \\ \mu & -\mu' & N \end{bmatrix} \begin{bmatrix} j & j & k' \\ \nu & -\nu' & N' \end{bmatrix} \begin{bmatrix} k & k' & K \\ q & -q' & Q \end{bmatrix} \\ &\quad \times \begin{bmatrix} k & k' & K \\ N & -N' & Q' \end{bmatrix} \int_0^\infty db \int d^3v_R n_p b v_R f_p(\vec{v}_e + \vec{v}_R) \mathfrak{D}_{QQ'}^K(\Omega_1) M_{\mu\mu'}^{\nu\nu'}(b, v_R, \Omega_0). \end{aligned} \quad (10)$$

Because of the axial symmetry,  $\bar{\Gamma}_{qq'}^{hh'}$  vanishes when  $q \neq q'$ ; then only the terms with  $Q = 0$  give rise to non-zero contributions to the summation on the right-hand side of Eq. (10). For the sake of simplicity, we denote  $\bar{\Gamma}_{qq'}^{hh'}$  by  $\bar{\Gamma}_q^{hh'}$ . After integrating  $\bar{\Gamma}_{qq'}^{hh'}$  over angle, one can see that only the terms with  $Q' = 0$  give rise to nonzero contributions (see Appendix A). Thus we obtain

$$\begin{aligned} \bar{\Gamma}_q^{hh'}(v_e) &= - \sum (-1)^{h+h'-q+\nu-\mu'} [(2k+1)(2k'+1)]^{1/2} (2K+1) \begin{bmatrix} j & j & k \\ \mu & -\mu' & N \end{bmatrix} \begin{bmatrix} j & j & k' \\ \nu & -\nu' & N \end{bmatrix} \\ &\quad \times \begin{bmatrix} k & k' & K \\ N & -N & 0 \end{bmatrix} \begin{bmatrix} k & k' & K \\ N & -N & 0 \end{bmatrix} \bar{\mathfrak{M}}_{\mu\mu',K}^{\nu\nu'}(v_e), \end{aligned} \quad (11a)$$

where

$$\begin{aligned} \bar{\mathfrak{M}}_{\mu\mu',K}^{\nu\nu'}(v_e) &= n_p \int_0^\infty db \int d^3v_R b v_R f_p(\vec{v}_e + \vec{v}_R) \\ &\quad \times P_K(\cos\theta) M_{\mu\mu'}^{\nu\nu'}(b, v_R, \Omega_0), \end{aligned} \quad (11b)$$

and  $P_K(\cos\theta) [= \mathfrak{D}_{00}^K(\Omega_1)]$  is the Legendre polynomial. The quadrupole integral in Eq. (11b) can be reduced to a simple infinite series (see Appendix A). We obtain for resonant collisions

$$\bar{\mathfrak{M}}_{\mu\mu',K}^{\nu\nu'}(v_e) = (-2)^K M_{\mu\mu'}^{\nu\nu'} \exp(-\alpha_p v_e^2) \times \sum_{m=0}^{\infty} \frac{(m+K)! \Gamma(m + \frac{1}{2}K + \frac{3}{2})}{(2m+2K+1)! m! \Gamma(\frac{3}{2})} (4\alpha_p v_e^2)^{m+K/2}, \quad (12a)$$

where  $\Gamma(x)$  is the  $\gamma$  function and  $M_{\mu\mu'}^{\nu\nu'}$  is defined in Eq. (A5a). For nonresonant collisions,

$$\bar{\mathfrak{M}}_{\mu\mu',K}^{\nu\nu'}(v_e) = (-2)^K M_{\mu\mu'}^{\nu\nu'} \exp(-\alpha_p v_e^2) \times \sum_{m=0}^{\infty} \frac{(m+K)! \Gamma(m + \frac{1}{2}K + \frac{9}{5})}{(2m+2K+1)! m! \Gamma(\frac{9}{5})} (4\alpha_p v_e^2)^{m+K/2}, \quad (12b)$$

where  $M_{\mu\mu'}^{\nu\nu'}$  is defined in Eq. (A5b).

It is readily verified that  $\bar{\Gamma}_q^{hh'}$  satisfies the following relations<sup>8</sup> from the invariance under reflection on planes containing the  $Z$  axis:

$$\bar{\Gamma}_q^{hh'} = (-1)^{h+h'} \bar{\Gamma}_{-q}^{hh'}, \quad (13a)$$

and from the hermiticity of density matrix  $\rho$ ,

$$\bar{\Gamma}_q^{hh'} = \bar{\Gamma}_{-q}^{h'h*}. \quad (13b)$$

From these two relations, we see that  $\bar{\Gamma}_q^{hh'}$  is real for even  $h+k'$ , imaginary for odd  $h+k'$ , and that  $\bar{\Gamma}_0^{hh'} = 0$  for odd  $h+k'$ . Furthermore, as we use the approximations of the electrostatic interaction and classical linear path and the one-level perturber approximation,<sup>8</sup> the system is invariant with time reversal, which yields

$$\bar{\Gamma}_q^{hh'} = (-1)^{h+h'} \bar{\Gamma}_q^{h'h*}. \quad (13c)$$

From Eqs. (13a)–(13c), we obtain

$$\bar{\Gamma}_q^{hh'} = \bar{\Gamma}_q^{h'h}. \quad (13d)$$

Numerical calculation of the elements of the relaxation matrix was made for the emitter state with total angular momentum  $j=1$  perturbed by nonresonant collisions. For nonresonant collisions,  $M_{mm'}^{nn'}(b, v_R, \Omega_0)$  may be shown to be a function of  $\xi (=B/b^5 v_R)$ , where  $B$  is the constant determined by the oscillator strengths for virtual transitions of emitter and perturber defined in Ref. 4 (see Appendix A). We have solved the Schrödinger equation in order to obtain  $M_{mm'}^{nn'}(\xi, \Omega_0)$

$[=M_{mm'}^{nn'}(b, v_R, \Omega_0)]$  for a single collision in the reference frame using the same procedure as in Ref. 4. Namely, we use the perturbation method in the region  $0.0 \leq \xi \leq 0.01$ , and we carried out the machine calculation with the Runge-Kutta-Gill method in the region  $0.01 \leq \xi \leq 5.0$ . In the region  $5.0 \leq \xi < \infty$ , we have obtained the solutions in the form of exponential asymptotic averages. {For isotropic collisions, only five elements,  $M_{00}^{00}(\xi, \Omega_0)$ ,  $M_{00}^{11}(\xi, \Omega_0)$ ,  $M_{11}^{11}(\xi, \Omega_0)$ ,  $\text{Re}[M_{10}^{10}(\xi, \Omega_0)]$ , and  $M_{-1-1}^{11}(\xi, \Omega_0)$ , are required essentially, and other elements which give rise to nonzero contributions are deduced from these five elements. In addition to these five elements,  $\text{Im}[M_{10}^{10}(\xi, \Omega_0)]$  is required for anisotropic collisions.} The values of  $M_{mm'}^{nn'}$  obtained by numerical integration of  $M_{mm'}^{nn'}(\xi, \Omega_0)$  over  $\xi$  are tabulated in Table I. Similar calculations have been made by Chamoun *et al.*<sup>10</sup> and the values of  $M_{mm'}^{nn'}$  are shown in a different basis from ours. The values calculated from the values in Table I in Ref. 10 by changing the basis are also shown in Table I. Similarly, Berman and Lamb<sup>4</sup> have shown the values averaged over all of collision directions for isotropic collisions. Since some of the averaged elements become zero from the spherical symmetry, we cannot get enough information to calculate the values of  $M_{mm'}^{nn'}$  in our basis. However, translating inversely our values into their basis and averaging them over the collision directions, we can see a good agreement with their values (within 0.1%).

Substituting the values in Table I into Eq. (12), we obtain the elements of the relaxation matrix  $\bar{\Gamma}_q^{hh'}$  as functions of an emitter velocity whose direction is fixed in the  $Z$  direction (Fig. 3). For isotropic collisions ( $\vec{v}_e = 0$ ),  $\bar{\Gamma}_q^{hh'}$  is diagonal with respect to  $k$  and is independent of  $q$  for each value of  $k$ . The appearance of nondiagonal components of the relaxation matrix and the splitting of the diagonal components (the relaxation rates of multipole components) with different values of  $|q|$  are due to the anisotropy of the velocity distribution, while it should be noted that the increase in the relaxation rates is due mainly to the increase

TABLE I. Averaged relaxation-matrix elements for nonresonant collisions in units of  $\frac{2}{5} \pi n_p B^{2/5} \langle v_p^3/5 \rangle$ , together with the values calculated by Chamoun *et al.*

	$M_{00}^{00}$	$M_{00}^{11}$	$M_{11}^{11}$	$\text{Re}(M_{10}^{10})$	$\text{Im}(M_{10}^{10})$	$M_{-1-1}^{11}$
Present work	-2.21	1.11	-5.38	-5.38	2.12	4.27
Chamoun <i>et al.</i> <sup>a</sup>	-2.11	1.05	-4.93	-4.51	1.58	3.36

<sup>a</sup>Reference 10.

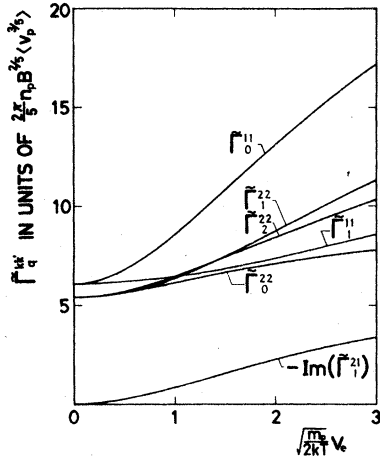


FIG. 3. Relaxation-matrix elements for emitters moving with a definite velocity in the  $Z$  direction as functions of the emitter velocity normalized by  $(2kT/m_e)^{1/2}$ .

in relative velocity rather than to the anisotropy.

#### B. Collisions of emitters excited by a single-mode laser

In the next stage, Eq. (11a) must be averaged over the velocity distribution of the excited emitters. In case of optical pumping with a laser beam, which has only axial symmetry, the velocity distribution is no longer isotropic. The axially symmetric situation induces a coupling between different tensorial orders, while it causes no coup-

ling between multipole components with different  $q$  if quantized along the axis of symmetry, as shown in Sec. IIIA.

We consider a single-mode laser beam propagated along the  $z$  direction with frequency  $\omega_L$ . This laser beam excites selectively the emitters whose axial velocity component  $v_{ez}$  is equal to  $v_0 \{= c [(\omega_L/\omega_0) - 1]\}$ , where  $\omega_0$  is the resonant frequency of the emitter transition. We shall consider only the case where the distribution function of  $v_{ez}$  can be regarded approximately as a  $\delta$  function, while the distribution of perpendicular component of  $v_e$  is Maxwellian. In this case the distribution of emitters can be expressed as

$$f_e(\vec{v}_e) = (\alpha_e/\pi) \exp[-\alpha_e(v_e^2 - v_0^2)] \delta(v_{ez} - v_0), \quad (14)$$

where  $\alpha_e = m_e/2kT$ ,  $m_e$  is the mass of the emitter, and the factor  $(\alpha_e/\pi) \exp(\alpha_e v_0^2)$  is the normalization constant.

The relaxation matrix for emitters whose velocity is in the direction of the polar angle  $(\Theta, \Phi)$  in the laboratory frame  $(x, y, z)$  can be obtained from Eq. (11a) through a rotation  $\Omega_2 = (\Phi, \Theta, 0)$  (see Fig. 4). Averaging over the emitter distribution, we obtain the averaged relaxation matrix:

$$\Gamma_{qq'}^{hh'}(v_0) = \sum_{q_1} \int d^3v_e f_e(\vec{v}_e) \mathfrak{D}_{q_1}^h(\Omega_2) \times \bar{\Gamma}_{q_1}^{hh'}(v_e) \mathfrak{D}_{q_1}^{h'}(\Omega_2). \quad (15)$$

From the axial symmetry of the system, we see that  $\Gamma_{qq'}^{hh'}$  vanishes when  $q \neq q'$ , as described above; we then obtain

$$\Gamma_q^{hh'}(v_0) = \sum_{Lq_1} (-1)^{q-q_1} (2L+1) \begin{bmatrix} k & k' & L \\ q & -q & 0 \end{bmatrix} \begin{bmatrix} k & k' & L \\ q_1 & -q_1 & 0 \end{bmatrix} \int d^3v_e f_e(\vec{v}_e) P_L(\cos\Theta) \bar{\Gamma}_{q_1}^{hh'}(v_e). \quad (16)$$

Substituting Eq. (11a) into Eq. (16), and after some algebra, we obtain

$$\Gamma_q^{hh'}(v_0) = - \sum (-1)^{k+k'-q+\nu-\mu'} [(2k+1)(2k'+1)]^{1/2} (2K+1) \begin{bmatrix} j & j & k \\ \mu & -\mu' & N \end{bmatrix} \begin{bmatrix} j & j & k' \\ \nu & -\nu' & N \end{bmatrix} \begin{bmatrix} k & k' & K \\ N & -N & 0 \end{bmatrix} \times \begin{bmatrix} k & k' & K \\ q & -q & 0 \end{bmatrix} \mathfrak{M}_{\mu\mu'K}^{\nu\nu'}(v_0), \quad (17a)$$

where

$$\mathfrak{M}_{\mu\mu'K}^{\nu\nu'}(v_0) = \int d^3v_e f_e(\vec{v}_e) P_K(\cos\Theta) \bar{\mathfrak{M}}_{\mu\mu'K}^{\nu\nu'}(v_e). \quad (17b)$$

Since  $\bar{\mathfrak{M}}_{\mu\mu'K}^{\nu\nu'}(v_e)$  consists of a quadruple integral, as seen in Eq. (11b), Eq. (17b) actually contains a sevenfold integral. Nevertheless, this can be

reduced to an infinite series with respect to  $x$  [ $= m_p/(m_p + m_e)$ ] (see Appendix B). For resonant collisions,

$$\mathfrak{M}_{\mu\mu'K}^{\nu\nu'}(v_0) = M_{\mu\mu'}^{\nu\nu'} \sum_{m=0}^{\infty} \frac{(m+K)! \Gamma(m + \frac{1}{2}K + \frac{3}{2})}{(2m+2K+1)! m! \Gamma(\frac{3}{2})} G_{mK}(v_0), \quad (18a)$$

and for nonresonant collisions,

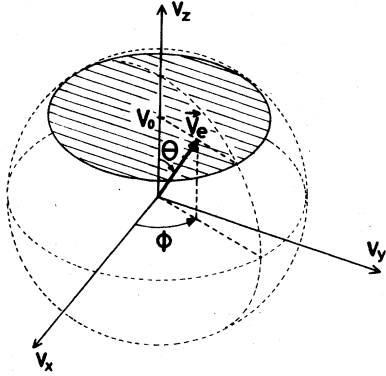


FIG. 4. Considered velocity distribution of emitters excited by a single-mode laser beam propagated along the  $z$  axis (shaded portion). The velocity distribution perpendicular to the  $z$  axis is given by a Maxwellian.

$$\mathfrak{M}_{\mu\mu'}^{\nu\nu'}(v_0) = M_{\mu\mu'}^{\nu\nu'} \sum_{m=0}^{\infty} \frac{(m+K)! \Gamma(m + \frac{1}{2}K + \frac{\theta}{2})}{(2m+2K+1)! m! \Gamma(\frac{\theta}{2})} G_{mK}(v_0), \quad (18b)$$

where

$$G_{mK}(v_0) = (-4)^K (1-x) \left( \frac{x}{1-x} \right)^{K/2} \zeta^K e^{\zeta^2} \times \sum_{r=0}^{\lfloor K/2 \rfloor} \frac{(2K-2r-1)!!}{r!(K-2r)!} \left( \frac{-1-x}{2\zeta^2} \right)^r \times \Gamma\left(m+r+1, \frac{\zeta^2}{1-x}\right) (4x)^m. \quad (18c)$$

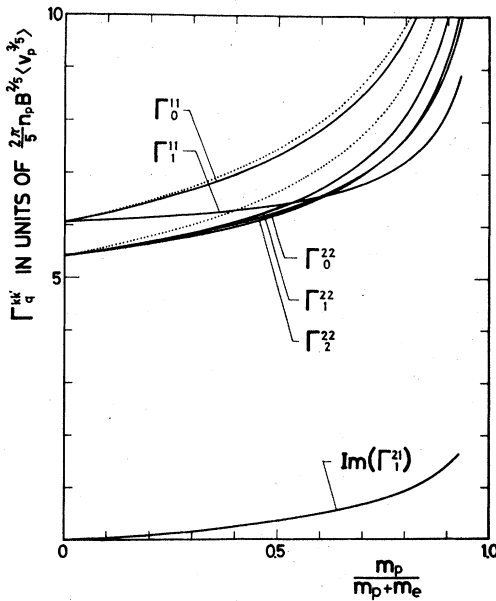


FIG. 5. Relaxation-matrix elements for emitters excited by a single-mode laser tuned to the center of the absorption line, as functions of  $x \equiv m_p / (m_p + m_e)$ . Two dotted curves show the case where emitters have an isotropic Maxwellian distribution.

In Eqs. (18),  $\zeta$  is given by  $\zeta = \sqrt{\alpha_e} v_0$ , which is proportional to the  $z$  component of the emitter velocities, and hence to the detuning of the incident laser frequency from the center frequency of the emitter transition;  $\Gamma(n, x)$  is the incomplete  $\gamma$  function.<sup>11</sup>

Because the whole system has the same symmetry as in Sec. IIIA, relations (13) are still valid for  $\Gamma_q^{hh'}$ . Substituting the values given in Table I into Eq. (18b) and using Eq. (17a), we obtain the elements of relaxation matrix  $\Gamma_q^{hh'}$  for the excited state with  $j=1$  perturbed by nonresonant collisions in the case of single-mode laser excitation. The infinite series in Eq. (18b) is convergent if  $0 \leq x < 1$ . This condition is always satisfied, but the convergence becomes worse when the mass of perturber is much larger than that of emitter ( $x \approx 1$ ). In Fig. 5, the components of the relaxation matrix for emitters excited by a single-mode laser tuned to the line center are shown as a function of  $x$  [ $\equiv m_p / (m_p + m_e)$ ]. In this case, only the emitters whose axial velocities are equal to zero are excited. As seen in Fig. 5, the relaxation rates  $\Gamma_q^{hh}$  in this case are smaller than those values for the isotropic case, which are shown by dotted curves. This is not surprising because the average relative velocity of emitters excited by a zero-detuning laser is smaller than that of isotropically excited emitters.

Figures 6 show the components of the relaxation matrix as a function of the axial emitter velocity, which is proportional to the detuning of the single-mode laser frequency. The relaxation rates of alignment and orientation for isotropic collisions are shown by two dotted lines. The transfer rates between alignment and orientation, which are pure imaginary, change their signs when the detuning is increased. It is worthwhile noting that all the relaxation-matrix elements are approximately equal to those for isotropic collisions when one detunes the laser frequency so that the axial velocity of the emitter is equal to 60–70% of  $(2kT/m_e)^{1/2}$ . It should be noted that, when the matrix elements shown in Figs. 6 are averaged with respect to  $v_0$  over the one-dimensional Maxwellian  $(m_e/2kT) \exp(-m_e v_0^2/2kT)$ , the diagonal elements are reduced to the relaxation rates for isotropic collisions and the off-diagonal elements are reduced to zero, as one might expect.

#### IV. OBSERVATION OF TRANSFER BETWEEN ALIGNMENT AND ORIENTATION

The above-mentioned effect of anisotropic collisions may be investigated by the observation of the collisional broadening in various experiments (e.g., Hanle effect, magnetic resonance, etc.).

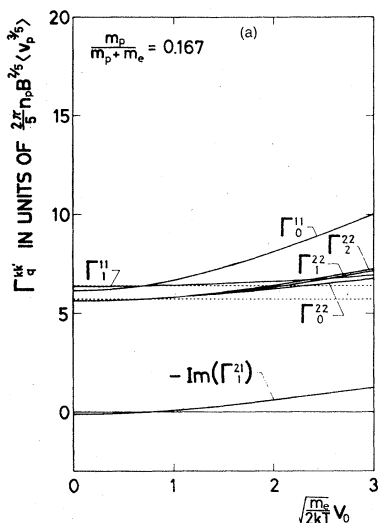


FIG. 6(a). Relaxation-matrix elements for emitters excited by a single-mode laser as functions of the normalized axial emitter velocity for  $x=0.167$ , which corresponds to the case of neon atoms perturbed by helium atoms.

In laser optical-pumping experiments with a single-mode laser, the anisotropy of velocity distribution is not, however, so large that the effect of anisotropic collisions on the broadening of the Hanle curve or magnetic resonance signal may not be so remarkable.

On the other hand, the transfer between alignment and orientation, which is absent in isotropic

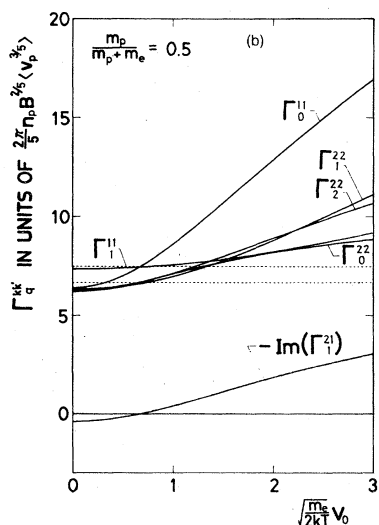


FIG. 6(b). Same as for Fig. 6(a), but for  $x=0.5$ , which corresponds to the case of nonresonant collisions of the same species.

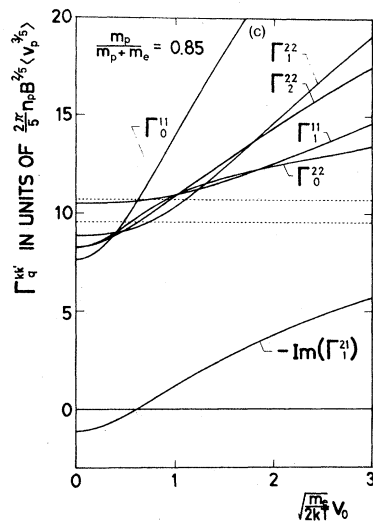


Fig. 6(c). Same as Fig. 6(a), but for  $x=0.85$ , which corresponds to the case of sodium atoms perturbed by xenon atoms.

collisions, increases with increasing degree of anisotropy. The averaged collisional interaction, which is discussed in preceding sections, has alignmentlike symmetry which is the same as the symmetry of the system in an electric field. When the excited atoms are aligned in a direction neither parallel nor perpendicular to the axis of anisotropy, orientation is created in the direction perpendicular to the plane which contains the alignment and the axis of anisotropy.<sup>12</sup> Conversely, when the excited atoms are oriented in a direction which is not parallel to the axis of anisotropy, alignment is created by collisions in the plane containing the axis of anisotropy, which is perpendicular to the plane containing both of the axes of orientation and anisotropy. In this plane, the direction of created alignment is neither parallel nor perpendicular to the axis of anisotropy.

Chamoun *et al.*<sup>10</sup> investigated the former effect, observing partially circularly polarized fluorescences from excited He atoms aligned by collisions with a heavy-ion beam. However, in such experiments using excitation by collisions, it is impossible to create orientation. In laser optical-pumping experiments, it is possible to create alignment and orientation of emitters by linearly and circularly polarized light beams respectively, and the degree of anisotropy can easily be changed by changing the detuning of the laser frequency. Thus it is possible to observe both transfer from alignment to orientation and from orientation to alignment.

In a weak magnetic field, the evolution of the density matrix can be expressed on the basis of

normalized irreducible tensors. As in the previous sections, we will take the axis of quantization parallel to the axis of anisotropy, i.e., parallel to the laser beam, not to the direction of the magnetic field. The density matrix for the  $q$  component of the  $2^k$ -pole moment is governed by

$$\frac{d\rho_q^k}{dt} = -i[\mathcal{H}, \rho]_q^k - \gamma_{\text{nat}} \rho_q^k - \sum_{k'} \Gamma_q^{kk'} \rho_q^{k'} + F_q^k. \quad (19)$$

The first term describes the interaction with the magnetic field  $\vec{H}$ :

$$[\mathcal{H}, \rho]_q^k = -g\mu_B \{ [k(k+1) - q(q-1)]/2 \}^{1/2} H_1 \rho_{q+1}^k - q H_0 \rho_q^k - \{ [k(k+1) - q(q+1)]/2 \}^{1/2} H_{-1} \rho_{q-1}^k, \quad (20)$$

where  $g$  is the  $g$  factor,  $\mu_B$  is the Bohr magneton, and

$$H_1 = -(H_x + iH_y)/\sqrt{2}, \quad H_0 = H_z, \quad H_{-1} = (H_x - iH_y)/\sqrt{2}. \quad (21)$$

The second and third terms in the right-hand side of Eq. (19) describe the relaxations due to spontaneous decay and to collisions, respectively. The last term describes the atomic state created by laser excitation from a lower state with total angular momentum  $j_g$  to the excited state with  $j$ :

$$F_q^k = (-1)^{j+j_g} \sqrt{2k+1} |\langle j || d || j_g \rangle|^2 \begin{Bmatrix} 1 & 1 & k \\ j & j & j_g \end{Bmatrix} \times F'_0 \Phi_q^k(\vec{k}, \lambda), \quad (22)$$

where  $\langle j || d || j_g \rangle$  is the reduced matrix element of the dipole moment operator,  $F'_0$  is a constant proportional to the light intensity, and  $\Phi_q^k$  is defined as<sup>13</sup>

$$\Phi_q^k = \sum_{q_1, q_2} (-1)^{q_2} e_{q_1} (e_{q_2})^* \begin{Bmatrix} 1 & 1 & k \\ q_1 & -q_2 & -q \end{Bmatrix}, \quad (23)$$

where  $e_q$  is the circular component of the polarization vector  $\vec{e}$  of the excitation light.

In Eq. (23), higher order effects of the laser excitation are neglected, and the Zeeman splittings of the excited and ground states are assumed to be much smaller than the Doppler width. The latter condition is satisfied in such ordinary experiments as the Hanle experiments, where the applied magnetic field is weak.

#### A. Excitation with linearly polarized light

When the laser beam propagated in the  $z$  direction is linearly polarized and  $\vec{H}$  is directed along the  $x$  axis, only the excitations  $F_0^0, F_0^2, \text{Re}(F_{\pm 2}^2)$ , and  $\text{Im}(F_{\pm 2}^2)$  are different from zero, as seen from Eq. (22) and Eq. (23). We then obtain the stationary solutions of Eq. (19) as

$$\begin{aligned} \text{Re}(\rho_1^1) &= -\frac{1}{\Delta_1} \Gamma \omega A, \quad \rho_0^1 = -\frac{\sqrt{2}}{\Delta_2} \Gamma \omega^2 \text{Im}(F_2^2), \\ \rho_0^2 &= \frac{1}{\gamma_0^2} F_0^2 - \frac{\sqrt{6}}{\Delta_1} \frac{\gamma_1^1}{\gamma_0^2} \omega^2 A, \quad \text{Im}(\rho_1^1) = -\frac{1}{\Delta_2} \gamma_0^1 \Gamma \omega \text{Im}(F_2^2), \\ \text{Im}(\rho_1^2) &= -\frac{1}{\Delta_1} \gamma_1^1 \omega A, \quad \text{Re}(\rho_1^2) = \frac{1}{\Delta_2} \omega (\gamma_0^1 \gamma_1^1 + \omega^2) \text{Im}(F_2^2), \\ \text{Re}(\rho_2^2) &= \frac{1}{\gamma_2^2} \text{Re}(F_2^2) - \frac{1}{\Delta_1} \frac{\gamma_1^1}{\gamma_2^2} \omega^2 A, \\ \text{Im}(\rho_2^2) &= \frac{1}{\Delta_2} [\gamma_1^2 (\gamma_0^1 \gamma_1^1 + \omega^2) + \gamma_0^1 \Gamma^2] \text{Im}(F_2^2), \end{aligned} \quad (24)$$

where

$$\begin{aligned} \Delta_1 &= (3\gamma_2^2 + \gamma_0^2) \gamma_1^1 \omega^2 + \gamma_0^2 \gamma_2^2 (\gamma_1^1 \gamma_1^2 + \Gamma^2), \\ \Delta_2 &= (\gamma_0^1 \gamma_1^1 + \omega^2) (\gamma_1^2 \gamma_2^2 + \omega^2) + \gamma_0^1 \gamma_2^2 \Gamma^2, \\ A &= \gamma_0^2 \text{Re}(F_2^2) + \frac{1}{2} \sqrt{6} \gamma_2^2 F_0^2, \\ \omega &= g\mu_B H, \quad \gamma_q^k = \gamma_{\text{nat}} + \Gamma_q^{kk}, \quad i\Gamma = \Gamma_1^{21} = \Gamma_{-1}^{21} = \Gamma_{-1}^{12} = \Gamma_1^{12}. \end{aligned} \quad (25)$$

The intensity of the fluorescence emitted in the direction  $\vec{k}$  with polarization  $\lambda$  is<sup>13</sup>

$$I_{\vec{k}} = (-1)^{j+j_0} I_0 \sum_k \sqrt{2k+1} \begin{Bmatrix} 1 & 1 & k \\ j & j & j_0 \end{Bmatrix} \times \sum_q (-1)^q \rho_q^k \Phi_q^k(\vec{k}, \lambda), \quad (26)$$

where  $j_0$  is the total angular momentum of the state to which atoms terminate after emission, and  $I_0$  is the proportionality constant. It is easily found from Eq. (26) that, when we observe the difference in the intensity between right-handed and left-handed circularly polarized emissions, the transverse orientation  $\rho_1^1$  can be observed:

$$I_{\sigma^+} - I_{\sigma^-} = (-1)^{j+j_0} I_0 \begin{Bmatrix} 1 & 1 & 1 \\ j & j & j_0 \end{Bmatrix} 2 \text{Re}(\rho_1^1). \quad (27)$$

Substituting the stationary solution for  $\text{Re}(\rho_1^1)$  in Eq. (24) into Eq. (27), we obtain

$$I_{\sigma^+} - I_{\sigma^-} = (-1)^{j+j_0} I_0 \begin{Bmatrix} 1 & 1 & 1 \\ j & j & j_0 \end{Bmatrix} \times \frac{2\omega \Gamma A}{(3\gamma_2^2 + \gamma_0^2) \gamma_1^1 \omega^2 + \gamma_0^2 \gamma_2^2 (\gamma_1^1 \gamma_1^2 + \Gamma^2)}. \quad (28)$$

This intensity difference for circularly polarized emissions can be explained as follows. The transverse alignment  $A$  created by laser light precesses in the  $y$ - $z$  plane under the influence of  $\vec{H}$ . Then the alignment  $\rho_1^2$  is created along the direction  $(\frac{1}{4}\pi, \frac{1}{2}\pi)$ , which is neither parallel nor perpendicular to the  $z$  axis. The anisotropic collisions transfer the alignment  $\rho_1^2$  to the transverse orientation  $\rho_1^1$  directed along the  $x$  axis. As seen in Eq. (28), this orientation signal is in dispersion shape when



the magnetic field is swept through zero.

On the other hand, the difference in the intensities of linearly polarized emissions polarized along the  $z$  and  $y$  directions shows the ordinary Hanle signal in Lorentzian shape:

$$\begin{aligned} I_{\parallel} - I_{\perp} &= (-1)^{j+j_0} I_0 \left\{ \begin{matrix} 1 & 1 & 2 \\ j & j & j_0 \end{matrix} \right\} [\sqrt{\frac{3}{2}} \rho_0^2 + \text{Re}(\rho_2^2)] \\ &= (-1)^{j+j_0} I_0 \left\{ \begin{matrix} 1 & 1 & 2 \\ j & j & j_0 \end{matrix} \right\} \\ &\quad \times \frac{(\gamma_1^2 \gamma_1^2 + \Gamma^2) A}{(3\gamma_2^2 + \gamma_0^2) \gamma_1^2 \omega^2 + \gamma_0^2 \gamma_2^2 (\gamma_1^2 \gamma_1^2 + \Gamma^2)}. \end{aligned} \quad (29)$$

From Eqs. (28) and (29), the ratio of the orientation signal to the alignment signal depicted in Fig. 7 becomes

$$\frac{A_{\text{or}}}{A_{\text{al}}} = \frac{\left\{ \begin{matrix} 1 & 1 & 1 \\ j & j & j_0 \end{matrix} \right\}}{\left\{ \begin{matrix} 1 & 1 & 2 \\ j & j & j_0 \end{matrix} \right\}} \frac{|\Gamma|}{\gamma_1^2} \left( \frac{4\gamma_1^4 \gamma_0^2 \gamma_2^2}{(\gamma_1^2 \gamma_1^2 + \Gamma^2)(3\gamma_2^2 + \gamma_0^2)} \right)^{1/2}. \quad (30)$$

For instance, for  $j=1$  and  $j_0=0$ ,

$$\frac{A_{\text{or}}}{A_{\text{al}}} = \frac{|\Gamma|}{\gamma_1^2} \left( \frac{4\gamma_1^4 \gamma_0^2 \gamma_2^2}{(\gamma_1^2 \gamma_1^2 + \Gamma^2)(3\gamma_2^2 + \gamma_0^2)} \right)^{1/2}. \quad (31)$$

Furthermore, when the anisotropy is small ( $\gamma_0^2 \simeq \gamma_1^2 \simeq \gamma_2^2$ ,  $\Gamma \ll \gamma_0^2$ ), we obtain for  $j=1$  and  $j_0=0$

$$A_{\text{or}}/A_{\text{al}} \simeq |\Gamma|/\gamma_1^2. \quad (32)$$

#### B. Excitation with circularly polarized light

When the laser beam propagated along the  $z$  axis is circularly polarized and  $\vec{H}$  is directed along the  $x$  axis, only the longitudinal orientation  $F_0^1$  and alignment  $F_0^2$  are excited. Then the stationary

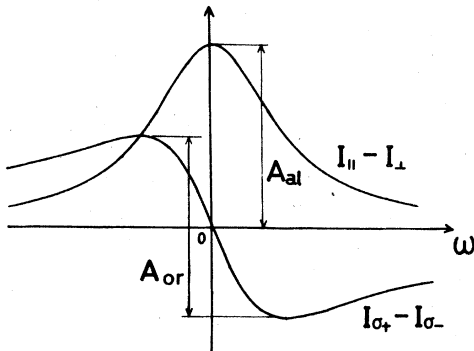


FIG. 7. Ordinary Hanle signal ( $I_{\parallel} - I_{\perp}$ ) and orientation signal ( $I_{\alpha+} - I_{\alpha-}$ ) as functions of  $\omega$  ( $\equiv g\mu_B H$ ) for excitation with a linearly polarized laser beam.

solutions of Eq. (19) are

$$\begin{aligned} \text{Re}(\rho_1^1) &= -\frac{\sqrt{6}}{2} \frac{1}{\Delta_1} \gamma_2^2 \Gamma \omega F_0^2, \\ \rho_0^1 &= \frac{1}{\Delta_2} [\gamma_1^2 \omega^2 + \gamma_2^2 (\gamma_1^2 \gamma_1^2 + \Gamma^2)] F_0^1, \\ \rho_0^2 &= \frac{1}{\gamma_0^2} F_0^2 - \frac{3}{\Delta_1} \frac{\gamma_1^4 \gamma_2^2}{\gamma_0^2} \omega^2 F_0^2, \\ \text{Im}(\rho_1^1) &= -\frac{\sqrt{2}}{2} \frac{1}{\Delta_2} \omega (\gamma_1^2 \gamma_2^2 + \omega^2) F_0^1, \\ \text{Im}(\rho_1^2) &= -\frac{\sqrt{6}}{2} \frac{1}{\Delta_1} \gamma_1^4 \gamma_2^2 \omega F_0^2, \quad \text{Re}(\rho_1^2) = -\frac{\sqrt{2}}{2} \frac{1}{\Delta_2} \gamma_2^2 \Gamma \omega F_0^1, \\ \text{Re}(\rho_2^2) &= -\frac{\sqrt{6}}{2} \frac{1}{\Delta_1} \gamma_1^4 \omega^2 F_0^2, \quad \text{Im}(\rho_2^2) = \frac{\sqrt{2}}{2} \frac{1}{\Delta_2} \Gamma \omega^2 F_0^1. \end{aligned} \quad (33)$$

In these results,  $\text{Re}(\rho_1^1)$ ,  $\rho_0^2$ ,  $\text{Im}(\rho_1^2)$ , and  $\text{Re}(\rho_2^2)$  show essentially the same results as before, because these results can be obtained as well by substituting  $F_2^2=0$  into Eq. (24). The solutions for  $\rho_0^1$  and  $\text{Im}(\rho_1^1)$  give the ordinary Hanle signal of orientation. It is  $\text{Re}(\rho_1^2)$  and  $\text{Im}(\rho_2^2)$  that show the transfer from orientation to alignment. From Eq. (26) it can be shown that, when we observe the fluorescence which is polarized linearly in the direction with the polar angle  $(\frac{1}{4}\pi, 0)$ , the intensity is given by

$$\begin{aligned} I &= (-1)^{j+j_0} I_0 \left[ \frac{1}{\sqrt{3}} \left\{ \begin{matrix} 1 & 1 & 0 \\ j & j & j_0 \end{matrix} \right\} \rho_0^0 \right. \\ &\quad \left. + \left\{ \begin{matrix} 1 & 1 & 2 \\ j & j & j_0 \end{matrix} \right\} \left( \frac{1}{2\sqrt{6}} \rho_0^2 - \text{Re}(\rho_1^2) + \frac{1}{2} \text{Re}(\rho_2^2) \right) \right]. \end{aligned} \quad (34)$$

When the sense of the circular polarization of the excitation is changed,  $F_0^1$  changes its sign, while  $F_0^2$  remains unchanged. Accordingly, the difference in the intensities of the fluorescence for the right- and left-handed circularly polarized excitations becomes

$$\begin{aligned} \Delta I &= I_0 \left\{ \begin{matrix} 1 & 1 & 1 \\ j & j & j_g \end{matrix} \right\} \left\{ \begin{matrix} 1 & 1 & 2 \\ j & j & j_0 \end{matrix} \right\} \\ &\quad \times \frac{\sqrt{2} \omega \gamma_2^2 \Gamma}{(\gamma_0^2 \gamma_1^2 + \omega^2)(\gamma_1^2 \gamma_2^2 + \omega^2) + \Gamma^2 \gamma_1^2 \gamma_2^2} F_0^1. \end{aligned} \quad (35)$$

If we neglect the small term  $\Gamma^2 \gamma_1^2 \gamma_2^2$  in the denominator, we can interpret Eq. (35) as follows. Circularly polarized light creates continuously the longitudinal orientation  $F_0^1$  in the  $z$  direction, which begins to precess in the  $y$ - $z$  plane under the influence of  $\vec{H}$  directed along the  $x$  axis. Consequently, the transverse orientation  $\rho_{\pm 1}^1$  is created in the  $y$  direction (the Hanle effect of orientation),  $\omega$  dependence of  $\rho_{\pm 1}^1$  being expressed as  $\omega/(\gamma_0^2 \gamma_1^2 + \omega^2)$ . This transverse orientation is transferred to the

transverse alignment  $\rho_{\pm 1}^2$  under the influence of anisotropic collisions with the transfer rate  $\Gamma$ . Furthermore, since this transverse alignment precesses about  $\vec{H}$ ,  $\rho_{\pm 1}^2$  is decreased by a factor of  $\gamma_2^2/(\gamma_1^2\gamma_2^2 + \omega^2)$  (the Hanle effect of alignment).

## V. DISCUSSION AND CONCLUSIONS

We have investigated the collisional relaxation among Zeeman substates for nonresonant collisions where the velocity distribution of emitters is anisotropic, especially in the case where the emitters are excited by a single-mode laser beam. Chamoun *et al.* observed the transfer from alignment to orientation in atoms excited by a heavy-ion beam,<sup>10</sup> and theoretically estimated this effect.<sup>14</sup> Their simple model of the emitter velocity distribution is not applicable to the case in which the emitters are excited by a single-mode laser. Here we shall summarize and discuss about the results obtained in the preceding sections.

The most remarkable feature of anisotropic collisions is the appearance of the transfer between alignment and orientation. It is shown in Figs. 5 and 6 that the transfer rate becomes larger with an increase in the ratio of the mass of perturber to that of emitter. Even when the single-mode laser is tuned to the line center, this transfer is sufficiently large to be observed experimentally. For example, the ratio of the transfer rate to the collisional broadening is about 6% when the mass of the emitter is equal to that of the perturber [i.e.,  $x \equiv m_p/(m_e + m_p) = 0.5$ ]. When the emitter is a sodium atom and the perturber is a xenon atom ( $x \approx 0.85$ ), this ratio amounts to about 12%, as seen in Fig. 5.

As the laser frequency is detuned from the line center, the transfer rate  $\Gamma_1^{21}$  begins to decrease, and at a detuning where the  $z$  component of normalized emitter velocity  $(m_e/2kT)^{1/2}v_0$  is 0.6–0.7, the transfer disappears. When the detuning is increased further, the transfer rate increases, with the sign opposite to that for the small detuning. This change of the sign of  $\Gamma_1^{21}$  appears as the change of the sign of the orientation signal in the experiment described in Sec. IV A, and as that of  $\Delta I$  in Sec. IV B.

Another feature of anisotropic collisions is the fact that the decay rate of a multipole moment  $\rho_q^k$  is also dependent on  $|q|$ . Furthermore, in the case of single-mode laser excitation, the decay rates increase as the detuning is increased. Therefore the decay rates obtained in the experiment with a single-mode laser are not the same as those for isotropic collisions. Even when the laser is tuned to the line center, the observed decay rates are smaller than those for isotropic

collisions. As one detunes the laser frequency from the absorption line center, the decay rates increase and finally become greater than the values for isotropic collisions. Consequently, it must be emphasized that one cannot in principle calculate the cross sections for destruction of multipole moments by comparing the experimental results with the isotropic collision theory. The error in the calculation of cross sections is, however, small when the perturber is not heavier than the emitter, and when the laser is tuned around the line center.

Although our calculations have been performed for the case where the distribution of  $v_{ez}$  is a  $\delta$  function, our results are applicable for an arbitrary distribution of  $v_{ez}$ . In this case, we can obtain the relaxation matrix  $\Gamma_q^{kk'}$  by integrating the relaxation matrix  $\Gamma_q^{kk'}(v_0)$  as follows:

$$\Gamma_q^{kk'} = \int_{-\infty}^{\infty} f(v_{ez}) \Gamma_q^{kk'}(v_{ez}) dv_{ez}, \quad (36)$$

where  $f(v_{ez})$  is the distribution of  $v_{ez}$ . For excitation with a multimode laser, the integral in Eq. (36) is reduced to a simple summation.

In Sec. IV of this paper, we have shown the effects of anisotropic collisions on the alignment and orientation signals, which can be obtained by sweeping the magnetic field through zero. In the case of the optical-rf double-resonance experiment, the shift of magnetic resonance line becomes important as well as its broadening. It has been shown by Happer<sup>15</sup> that a weak isotropic fluctuating perturbation in a strong magnetic field such that the Larmor precession cannot be neglected compared with the correlation time of the perturbation induces anisotropic relaxations of multipole moments and causes energy shifts of Zeeman substates as if a fictitious magnetic field were present. Recently Gay<sup>16</sup> has shown that, even if the velocity distribution is isotropic, similar shifts are caused by collisional perturbations in such a strong magnetic field. In the present case, the anisotropic relaxation is caused by the anisotropic velocity distribution of the emitter atoms, and hence the symmetry of the system is different from that of above cases. Namely, there is a symmetry with respect to the planes containing the laser beam, so that the symmetry of the present system is quite analogous to that of the system in an electric field, which induces the Stark shift. Consequently, it is expected that, when one considers the emitter atoms with  $j=1$ , the magnetic resonance line is decomposed into two components which are shifted to opposite directions with the same amount by the anisotropic relaxation. However, as the shifts are expected to be much smaller than the broadening of each component, the

overall resonance line to be observed might never split and have only one unshifted peak at the center.

#### ACKNOWLEDGMENT

This work was supported in part by the Ministry of Education, Japan, under a Grant-in-Aid for Scientific Research.

#### APPENDIX A

The averaging over  $\vec{v}_R$  in Eq. (10) is performed by using the transformation

$$\int d^3v_R \rightarrow \int_0^\infty v_R^2 dv_R \int_0^\pi \sin\theta d\theta \int_0^{2\pi} d\phi \int_0^{2\pi} d\psi.$$

Since the perturber velocity distribution function  $f_p(\vec{v}_e + \vec{v}_R)$  is symmetric with respect to the  $Z$  axis,  $f_p(\vec{v}_e + \vec{v}_R)$  is independent of  $\phi$  and  $\psi$ . The angular integration over  $\phi$  and  $\psi$  in Eq. (8) is easily performed by using the relation

$$\int_0^{2\pi} d\phi \int_0^{2\pi} d\psi \mathcal{D}_{Q^0}^K(\Omega_1) = 4\pi^2 \delta_{Q^0} \delta_{Q^0} P_K(\cos\theta), \quad (\text{A1})$$

where  $P_K$  is the Legendre polynomial. We have used the relation (A1) to obtain Eqs. (11a) and (11b). Substituting Eq. (6) into Eq. (11b), we obtain

$$\begin{aligned} \bar{\mathcal{M}}_{\mu\mu'}^{\nu\nu'} = 4\pi(\alpha_p/\pi)^{3/2} \exp(-\alpha_p v_e^2) \int_0^\infty v_R^2 dv_R \\ \times \exp(-\alpha_p v_R^2) F_K(2\alpha_p v_e v_R) \bar{M}_{\mu\mu'}^{\nu\nu'}(v_R), \end{aligned} \quad (\text{A2})$$

where

$$\begin{aligned} F_K(x) &= \frac{1}{2} \int_0^\pi \sin\theta d\theta \exp(-x \cos\theta) P_K(\cos\theta) \\ &= (-2)^K \sum_{m=0}^{\infty} \frac{(m+K)!}{(2m+2K+1)! m!} x^{2m+K}, \end{aligned} \quad (\text{A3})$$

and

$$\bar{M}_{\mu\mu'}^{\nu\nu'}(v_R) = 2\pi n_p \int_0^\infty db b v_R M_{\mu\mu'}^{\nu\nu'}(b, v_R, \Omega_0). \quad (\text{A4})$$

As seen in Berman's theory<sup>4</sup>, the dependence of  $M_{\mu\mu'}^{\nu\nu'}(b, v_R, \Omega_0)$  on  $b$  and  $v_R$  can be expressed in terms of a parameter  $\xi$  as  $M_{\mu\mu'}^{\nu\nu'}(\xi, \Omega_0) \equiv M_{\mu\mu'}^{\nu\nu'}(b, v_R, \Omega_0)$ .

For resonant collisions,  $\xi \equiv A/(b^2 v_R)$  and  $A \equiv (e^2/6\hbar) |\langle s||r||a \rangle|^2$ , where  $\langle s||r||a \rangle$  is the reduced matrix element for the real transition induced by a collision. From Eq. (A4), we can show that  $\bar{M}_{\mu\mu'}^{\nu\nu'}(v_R)$  is independent of  $v_R$  for resonant collisions:

$$\begin{aligned} \bar{M}_{\mu\mu'}^{\nu\nu'}(v_R) &= n_p \pi A \int_0^\infty M_{\mu\mu'}^{\nu\nu'}(\xi, \Omega_0) \xi^{-2} d\xi \\ &\equiv M_{\mu\mu'}^{\nu\nu'}. \end{aligned} \quad (\text{A5a})$$

For nonresonant collisions,  $\xi \equiv B/(b^5 v_R)$  and

$$B \equiv (e^4/36\hbar^2 \Delta\omega) |\langle s||r_e||a \rangle \langle s'||r_p||p \rangle|^2,$$

where  $\langle s||r_e||a \rangle$  and  $\langle s'||r_p||p \rangle$  are the reduced matrix elements for virtual transitions of emitter and perturber, respectively, and  $\Delta\omega$  is the energy difference in angular frequency units between the initial and intermediate states of the emitter-perturber system. From Eq. (A4), we can show that  $\bar{M}_{\mu\mu'}^{\nu\nu'}(v_R)$  depends on  $v_R$  for nonresonant collisions as follows:

$$\bar{M}_{\mu\mu'}^{\nu\nu'}(v_R) = [\sqrt{\pi}/2\Gamma(\frac{3}{5})] (\alpha_p v_R)^{3/10} M_{\mu\mu'}^{\nu\nu'}, \quad (\text{A5b})$$

where

$$M_{\mu\mu'}^{\nu\nu'} \equiv \frac{2}{5} \pi n_p B^{2/5} \langle v_p^{3/5} \rangle \int_0^\infty M_{\mu\mu'}^{\nu\nu'}(\xi, \Omega_0) \xi^{-7/5} d\xi.$$

The integration over  $\xi$  in Eqs. (A5) must be performed numerically. Equations (10) are easily obtained from Eqs. (A2) and (A5) by using  $\gamma$  functions.

#### APPENDIX B

In order to perform the averaging over  $\vec{v}_e$  in Eq. (17b), we introduce a function  $G_{mK}(v_0)$  defined as

$$\begin{aligned} G_{mK}(v_0) &\equiv (-2)^K \int d^3v_e f_e(\vec{v}_e) P_K(\cos\Theta) \\ &\quad \times \exp(-\alpha_p v_e^2) (4\alpha_p v_e^2)^{m+K/2}. \end{aligned} \quad (\text{B1})$$

Using the function  $G_{mK}(v_0)$ , we can rewrite Eq. (17b) as Eq. (18a) for resonant collisions and as Eq. (18b) for nonresonant collisions.

To obtain the explicit form of  $G_{mK}(v_0)$ , we substitute the emitter velocity distribution given by Eq. (14) into Eq. (B1). After integrating Eq. (B1) over  $\Phi$ , we obtain

$$\begin{aligned} G_{mK}(v_0) &= -(-2)^{K+1} \alpha_e \exp(\alpha_e v_0^2) \int_0^\infty v_e^2 dv_e \\ &\quad \times \int_0^\pi \sin\Theta d\Theta (4\alpha_p v_e^2)^{m+K/2} \exp[-(\alpha_e + \alpha_p) v_e^2] \\ &\quad \times \delta(v_e \cos\Theta - v_0) P_K(\cos\Theta). \end{aligned} \quad (\text{B2})$$

After integrating Eq. (B2) over  $\Theta$ , we obtain

$$\begin{aligned} G_{mK}(v_0) &= -(-2)^{K+1} \alpha_e (4\alpha_p)^{m+K/2} \\ &\quad \times \int_{v_0}^\infty dv_e v_e^{2m+K+1} \exp[-(\alpha_e + \alpha_p) v_e^2] P_K\left(\frac{v_0}{v_e}\right). \end{aligned} \quad (\text{B3})$$

It is convenient to expand the Legendre polynomial as

$$P_K(v_0/v_e) = \sum_{r=0}^{[K/2]} \frac{(2K-2r-1)!!}{(-2)^r r! (K-2r)!} (v_0/v_e)^{K-2r}, \quad (\text{B4})$$

where  $[K/2]$  is the largest integer that does not

exceed  $\frac{1}{2}K$ . Using Eq. (B4) and the incomplete  $\gamma$  function defined as  $\Gamma(n, x) = \int_x^\infty t^{n-1} e^{-t} dt$ , we obtain

$$G_{mK}(v_0) = (-4)^K (1-x) \left( \frac{x}{1-x} \right)^{K/2} \xi^2 e^{\xi^2} \sum_{r=0}^{[K/2]} \frac{(2K-2r-1)!!}{r!(K-2r)!} \left( -\frac{1-x}{2\xi^2} \right)^r \Gamma\left(m+r+1, \frac{\xi^2}{1-x}\right) (4x)^m, \quad (\text{B5})$$

where  $x \equiv m_p / (m_e + m_p)$  and  $\xi \equiv (a_e)^{1/2} v_0$ .

<sup>1</sup>See Refs. 3, 4, 8, and 9, and references cited therein.

<sup>2</sup>See, for example, M. Dumont and B. Decomps, *J. Phys. (Paris)* **29**, 181 (1968); B. Decomps and M. Dumont, *ibid.* **29**, 443 (1968); M. Tsukakoshi and K. Shimoda, *J. Phys. Soc. Jpn.* **26**, 758 (1969).

<sup>3</sup>A. Omont, *J. Phys. (Paris)* **26**, 26 (1965).

<sup>4</sup>P. R. Berman and W. E. Lamb, *Phys. Rev.* **187**, 221 (1969).

<sup>5</sup>J. Cooper and D. N. Stacey, *Phys. Rev. A* **12**, 2438 (1975).

<sup>6</sup>M. E. Rose, *Elementary Theory of Angular Momentum* (Wiley, New York, 1957).

<sup>7</sup>We have used the definition used in Ref. 8, which differs from that used in Ref. 9 in its normalization.

<sup>8</sup>A. Omont, *Prog. Quantum Electron.* **5**, 69 (1977).

<sup>9</sup>M. I. D'yakonov and V. I. Perel', *Zh. Eksp. Teor. Fiz.* **48**, 345 (1965) [*Sov. Phys.-JETP* **21**, 227 (1965)].

<sup>10</sup>E. Chamoun, M. Lombardi, M. Carré, and M. I. Gaillard, *J. Phys. (Paris)* **38**, 591 (1977).

<sup>11</sup>F. Abramowitz and J. A. Stegun, *Handbook of Mathematical Functions* (Dover, New York, 1968).

<sup>12</sup>M. Lombardi, *J. Phys. (Paris)* **30**, 631 (1969).

<sup>13</sup>M. I. D'yakonov, *Zh. Eksp. Teor. Fiz.* **47**, 2213 (1964) [*Sov. Phys.-JETP* **20**, 1484 (1965)].

<sup>14</sup>M. Carré, M. L. Gaillard, and M. Lombardi, *J. Phys. (Paris)* **38**, 533 (1977).

<sup>15</sup>W. Happer, *Phys. Rev. B* **1**, 2203 (1970).

<sup>16</sup>J. C. Gay, *J. Phys. (Paris)* **37**, 1135 (1976); *ibid.* **37**, 1155 (1976).